Handling illumination for improved structural and quantitative interpretation

Laurence Letki, Maud Cavalca & Robin Fletcher, Schlumberger

In a complex environment, inadequate subsurface illumination due to complex geology or limitations of the acquisition geometry has detrimental effects on the amplitudes and phases of the migrated image. If left partially uncompensated for, such illumination effects will negatively impact both structural and quantitative interpretation results, leading to an imprint of non-geological effects in the resulting elastic parameters estimated by seismic inversion.

Least-square migration can help to efficiently mitigate illumination effects. Herein, we use least-squares migration schemes implemented in the image domain. Dip-dependent illumination effects due to complex geology and/or limitations of the acquisition geometry are captured using point-spread functions and corrected through inversion in the image domain. The resulting reflectivity image(s) show(s) higher-resolution events associated with more reliable amplitudes. The approach is also naturally extended to directly derive acoustic or elastic properties. These methods, therefore, enable improved structural and quantitative interpretation through correctly handling illumination effects.

This work reviews several variants of image-domain least-squares migration and illustrates their benefits through synthetic and field data examples from the Gulf of Mexico and Brazil Santos Basin.

Introduction

Complex geology, combined with limitations imposed by surface seismic acquisition geometries can lead to inadequate illumination of subsurface targets, which is detrimental to the amplitude and phase of the migrated image. Left partially uncorrected, such effects will negatively impact the interpretability of the images, which will also remain unsuitable for seismic attributes extraction, amplitude variation with offset (AVO) analysis, and amplitude inversion.

Least-squares migration (LSM) schemes can help to address this challenge. Data-domain LSM approaches can greatly improve the fidelity of our seismic depth images and common image gathers, and are increasingly thought to be worth the extra effort (Salomons et al., 2014). Alternately, as discussed by Fletcher et al. (2015), LSM schemes implemented in the image domain constitute a viable and possibly more cost-effective alternative to data-domain LSM.

We discuss the implementation of least-squares migration in the image domain (LSM-i), both in the context of Kirchhoff depth migration (KDM) and reverse time migration (RTM). We also illustrate the extension of these inversion schemes to recover earth model properties directly.

Capturing illumination using point-spread functions

The LSM-i workflow uses point-spread functions (PSFs) to capture and correct for space-, depth-, and dip-dependent illumination effects. PSFs are the impulse response of the modelling and imaging procedures. The image is considered to be modelled by performing a non-stationary convolution of the reflectivity model with the PSFs. The PSFs' grid can, therefore, be seen as a blurring operator, a measure of the illumination effects due to velocity variations and acquisition geometry that blurs the reflectivity to give the migrated image.

In a case study located in an area with a complex salt structure in the Gulf of Mexico (Letki et al., 2015a), we observe a clear imprint of the non-uniform illumination of the target subsalt horizon on the amplitudes of the corresponding event in the RTM image (Figure 1).

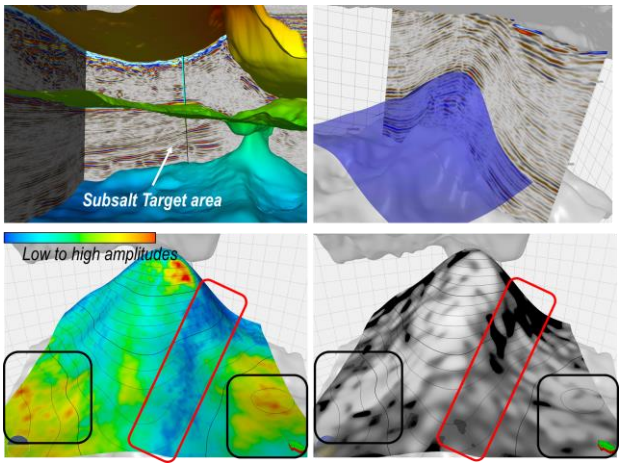

Figure 1 - *(top left) Illustration of the subsalt target area. (top right) RTM image with source illumination compensation with target horizon interpretation overlay. (bottom left) RMS amplitudes extracted around the target horizon. (bottom right) Illumination map at target horizon (from very low illumination in black to high illumination in white). Highlighted in red, the low-illumination corridor corresponds to a low-amplitude corridor in the RTM image. Highlighted in black, high amplitudes in the RTM image correspond to highly illuminated areas.*

PSFs can be generated using two-way wave-equation propagation to capture the illumination effects affecting the RTM image. The information captured by the PSFs can be correlated with the amplitude and phase variations observed along the target horizon, as illustrated in Figure 2. A PSF corresponding to an area with lower amplitudes in the RTM image was extracted and analysed. The spectra of the PSF strongly vary with dip. The geological dip estimated from the RTM image lies at the edge of the illuminated dip range. This observation confirms the strong imprint of the variable illumination on the RTM image.

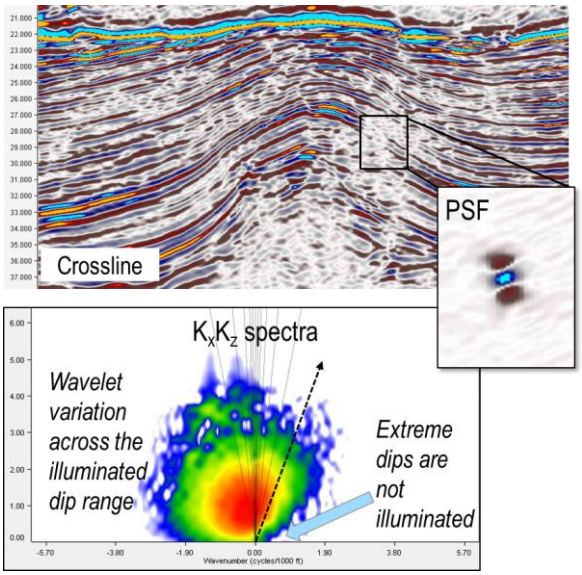

Figure 2 – *(top) Crossline through the RTM image. (middle) Crossline through a PSF extracted in a low-illumination area highlighted with the black box. (bottom) Associated wavenumber spectra showing the dip-dependent illumination effects captured by the PSF. The estimated local geological dip is represented by the black arrow.*

PSFs can also be generated using ray-based propagation to capture illumination effects affecting Kirchhoff depth-migrated images. (Figure 3). The method (Cavalca et al., 2016) uses two distinct sets of weighted Green's functions, characterizing the modelling process and the migration process.

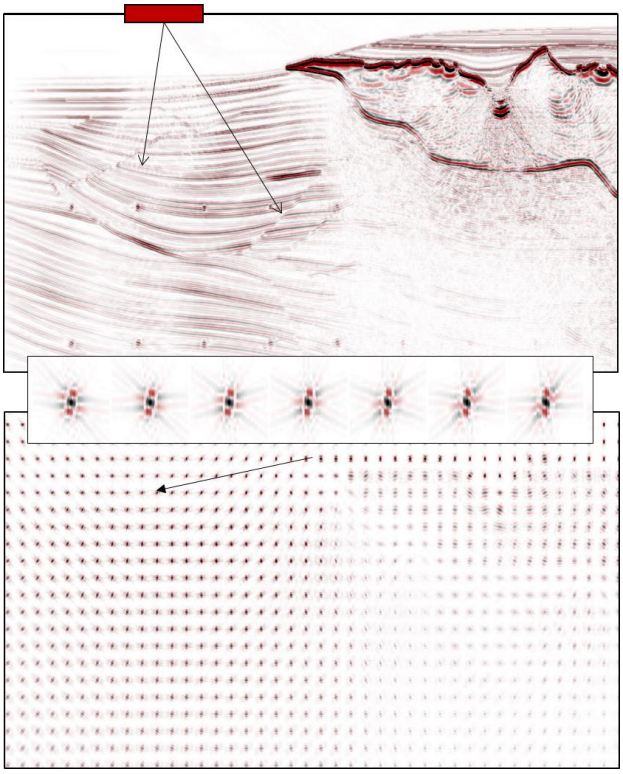

Figure 3 – *(top) KDM image using Sigsbee2A acoustic model and data, provided by the SMAART consortium. The acquisition geometry was randomly decimated in the location highlighted in red, leading to additional illumination effects in the image. (bottom) Corresponding volume of KDM PSFs - and (middle) zoom on a few PSFs - clearly showing the variable illumination due to the complex overburden (for example, below the salt) and the irregular acquisition geometry.*

For both RTM and KDM PSFs, simplification, optimization, and stabilization features that are now commonly embedded in the RTM or KDM production algorithms can be replicated to ensure full consistency between the PSFs and the corresponding seismic depth image. In the case of the KDM PSFs, this is achieved by modifying accordingly the migrated Green's functions and assigning appropriate migration weights during summation of all source/receiver pair contributions. This includes, for instance, antialiasing processes, mute functions, acquisition weighting schemes, and geometrical spreading corrections.

Conversely, the modelling process used to generate PSFs attempts to capture, to the best of our knowledge and capabilities, the effects of propagation in the earth that are not accounted for in preprocessing. Various propagation effects can be taken into account, even if, or all the more if, they were ignored or treated differently during the migration process. A specific example for KDM PSFs is the computation of geometrical spreading along the rays (through paraxial approximation) such that it is accurately captured in modelling Green's function.

Furthermore, including absorption effects and/or ghost effects in the modelling process enables PSFs to capture the amplitude- and phase-combined effects of illumination

and absorption (and/or ghost). These PSFs can then be used to compensate the migrated images for illumination and absorption effects (and/or ghost effects) simultaneously through the least-squares migration process (Caprioli et al., 2014: Cavalca et al., 2015).

Correcting for illumination effects using LSM-i

The LSM-i workflow finds the best reflectivity model by minimizing, in a least-squares sense, the difference between the image and a synthetic image derived through non-stationary convolution of the reflectivity model with the PSFs. Different level of preconditioning, regularization, and model constraints can be used during inversion. The output is a reflectivity image corrected for the illumination effects.

To limit computational and memory cost, PSFs are generated at a sparse set of subsurface locations. A PSF is then derived at each location in space by interpolating the grid of computed PSFs "on-the-fly" during application of the convolution operator. Note that the spatial and depth sampling of the PSF locations is particularly important. This sampling should be sufficient to resolve the variations embedded in the image.

In the Gulf of Mexico case study introduced above, comparisons of the initial RTM image and the LSM-i result (Figure 4) show a clear improvement in major event continuity, together with an overall bandwidth extension and sharpening of the image. Minor low-amplitude events, hard to see in the RTM image, are revealed in the reflectivity image derived with LSM-i. The amplitudes along the key horizons in the reflectivity image also appear more balanced and more consistent with the structure. Non-geological amplitude effects related to the variable illumination are nicely mitigated.

This case study also highlighted the fact that extra care is required close to hard boundaries. In the presence of such boundaries, we observe severe PSF variations across the discontinuity, most noticeably in the wavelet stretch and in differing dips illuminated. In this case, the linear interpolation assumption is no longer valid and the results will not be as reliable around such a strong contrast. This effect can be mitigated by increasing the density of PSFs and by implementing more adequate non-linear interpolation schemes.

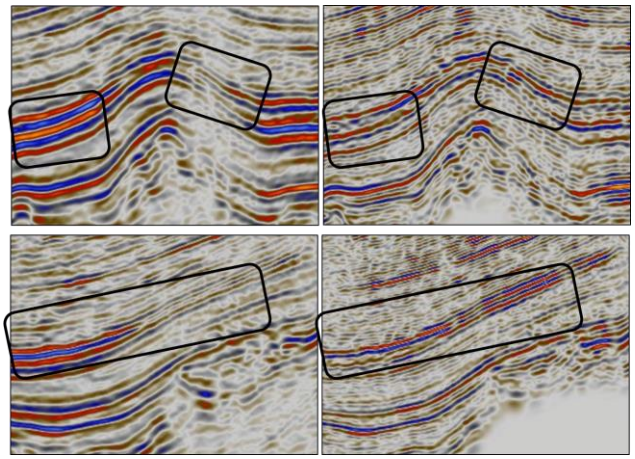

Figure 4 – *(left) RTM image with source illumination compensation. (right) Reflectivity image derived with LSM-i.*

In the context of Kirchhoff depth migration, the LSM-i workflow can be used to output the illumination-corrected reflectivity image from the original KDM stacked image (Figure 5). It can also be extended to a prestack implementation. In our experiment, we implement a prestack LSM-i scheme in the offset domain. We now seek the offset-dependent reflectivity model that minimizes, in a least-squares sense, the difference between the KDM offset gathers and synthetic offset gathers derived through non-stationary convolution of the offset-dependent reflectivity model with the PSFs at the corresponding offset. The output is illumination-corrected KDM offset gathers (Figure 6).

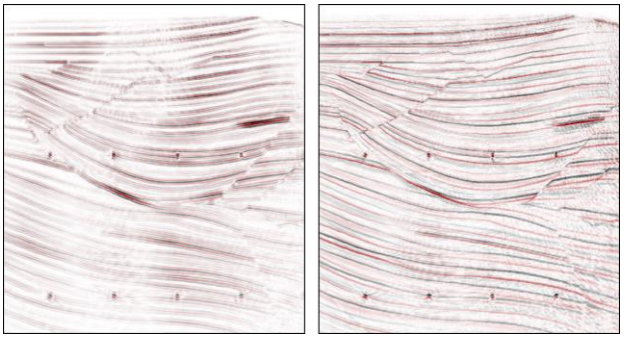

Figure 5 – *Poststack LSM-i example using the Sigsbee2A model and data. (left) Original KDM image impacted by illumination effects caused by complex overburden (presence of the salt body on the far right) and irregular decimated acquisition geometry. (right) Reflectivity image derived with LSM-i showing a good compensation of the dip-dependent illumination effects.*

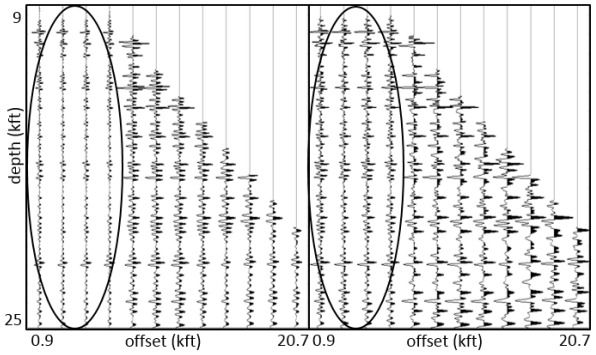

Figure 6 – *(left) KDM common image gather. The acquisition geometry was decimated (random decimation in different offset bins) creating a strong illumination imprint as a function of offset. (right) After LSM-i, the illumination effects are corrected and we recover the correct amplitude versus offset behavior.*

These illumination-corrected gathers would then be appropriate to form angle stacks for prestack inversion to elastic properties, leading to higher-fidelity rock properties.

Extension to depth-domain inversion

Although conventional inversion techniques can be applied to the improved imaging products obtained from LSM-i, a natural extension of the LSM-i workflow consists of directly generating - in addition to the reflectivity images - acoustic and elastic properties, corrected for illumination effects.

In this case, the reflectivity model is expressed as a function of the elastic earth model properties (using a linearized or full implementation of the Zoeppritz equations), and the inverse problem is parameterized using the elastic properties directly.

This workflow is referred to as depth-domain inversion (DDI). In this context, the PSFs can be seen as a representation of the space- and depth-variant 3D wavelet embedded in the migrated image that replaces the 1D wavelet used in conventional amplitude inversion. Well data are required to generate a low-frequency model and to calibrate the PSFs, such that the output of DDI is an absolute acoustic impedance volume, together with, in the prestack case, a Vp/Vs volume and a density volume. Note that the recovery of prestack properties remains conditional to the range of subsurface angles available.

Referring back to the case study from the Gulf of Mexico, Figure 7 compares the acoustic impedance volume obtained from the RTM image using a conventional time-domain inversion approach, with the results obtained from the depth-domain inversion approach. The variable illumination effects directly impact the time-domain inversion results, with low amplitudes being wrongly inverted into low reflectivity. The acoustic impedance volume derived through depth-domain inversion is corrected for these effects, leading to more consistent acoustic impedance layers. These results illustrate how depth-domain inversion can improve the fidelity of both structural and quantitative interpretation of complex subsalt targets.

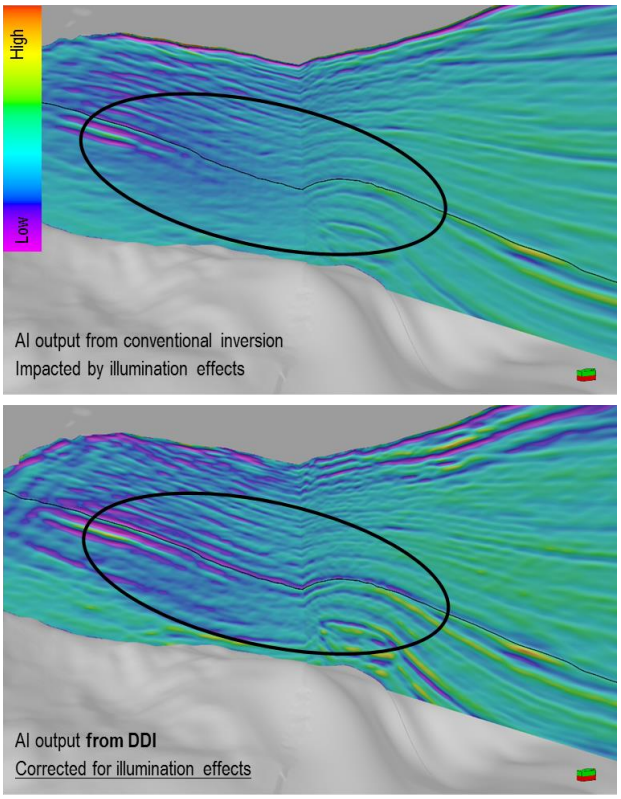

Figure 7 – *(top) Acoustic impedance volume derived with conventional time-domain inversion (converted back to depth for comparison purposes), and (bottom) acoustic impedance volume derived with depth-domain inversion, annotated with an interpretation of a key horizon. A comparison of the areas highlighted in the black ovals demonstrates how quantitative interpretation is improved after depth-domain inversion. (Includes data supplied by IHS Energy Log Services, Inc.; Copyright (2015) IHS Energy Log Services, Inc.)*

This technique has proved valuable in other complex salt environments, including the pre-salt area of the Brazil Santos Basin (Letki et al., 2015b). In this case, the benefits of the depth-domain inversion over time-domain inversion were particularly visible in areas of significant structural dip variations, such as in the layered salt. The PSFs successfully captured the dip-dependent illumination effects, leading to higher-fidelity acoustic impedance estimates in areas originally affected by strong dip-dependent wavelet effects (Figure 9).

The technique was also extended to perform AVO inversion of RTM source-direction gathers (Du et al., 2016) (Figure 8). In the approach, the subsurface angle, required for an accurate reflectivity calculation, is derived on-the-fly during the inversion process using the reflector's dip and azimuth estimated from a stacked image.

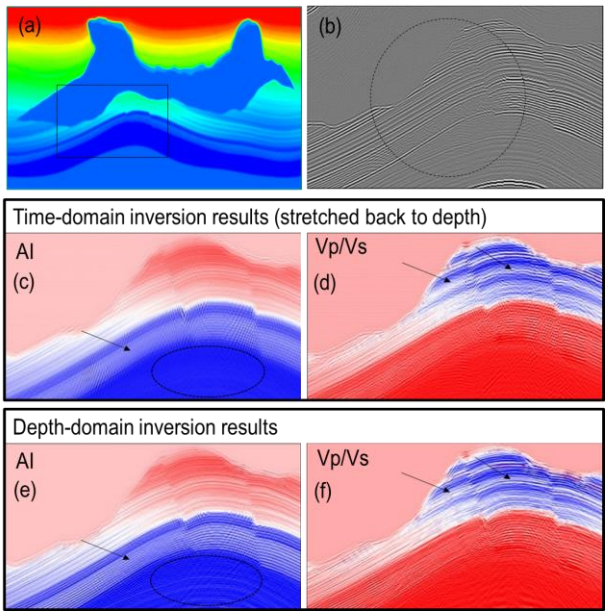

Figure 8 *– Example of pre-stack DDI results. (a) P-wave migration velocity model, (b) RTM stacked image in the target region, (c) Acoustic impedance and (d) Vp/Vs results from conventional time-domain inversion (stretched back to depth), (e) Acoustic impedance and (f) Vp/Vs results from depth-domain inversion.*

Conclusions

Least-squares migration in the image domain is a solution to capture the illumination effects affecting the image and retrieve the underlying subsurface reflectivity. This approach provides better event continuity, a sharper image, and more reliable amplitude information. It constitutes an interesting alternative to data-domain least-squares migration schemes and can be naturally extended to a direct estimation of the acoustic and elastic earth model properties.

These methods, therefore, enable improved structural and quantitative interpretation through the correct handling of illumination effects.

Acknowledgments

The authors thank WesternGeco for permission to publish this work and for permission to use the data.

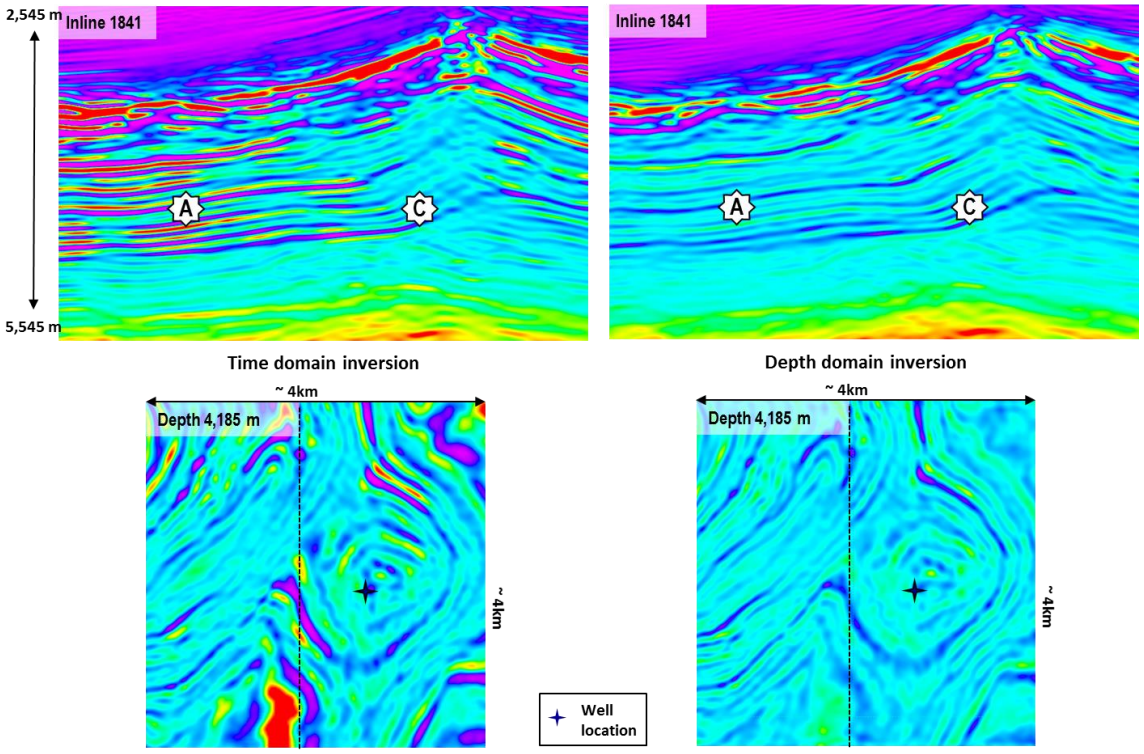

Figure 9 – *Example from Brazil Santos Basin. Comparison of time-domain inversion acoustic impedance result (stretched back to depth) and depth-domain inversion acoustic impedance result. In areas with significant structural dip variations, such as in the layered salt structure, the amplitude variations observed in the acoustic impedance volume from the conventional time-domain inversion (for example, at point A versus point C) are strongly correlated to the dip-dependent amplitude variations of the RTM image. The depth-domain inversion result shows an overall better balanced acoustic impedance and a reduced imprint of the RTM image amplitudes. (Taken from Letki et al., 2015b)*

References

Caprioli, P.B.A., Du, X., Fletcher, R.P., and Vasconcelos, I. 2014. 3D source deghosting after imaging. 84th Annual International Meeting, SEG, Expanded Abstracts, 4092-4096.

Cavalca, M., Fletcher, R.P. and Du X. 2015. Q-compensation through depth domain inversion. 77th EAGE Conference & Exhibition, Extended Abstracts.

Cavalca, M, Fletcher, R.P. and Caprioli, P. 2016. Least-Squares Kirchhoff Depth Migration in the image domain. 78th EAGE Conference & Exhibition, Expanded Abstracts.

Du, X., Fletcher, R.P. and Cavalca, M. 2016. Pre-stack depth domain inversion after reverse-time migration. 78th EAGE Conference & Exhibition, Extended Abstracts.

Fletcher, R.P., Nichols, D., Bloor, R., and Coates, R.T. 2015. Least-squares migration: data domain versus image domain. 77th EAGE Conference & Exhibition, Extended Abstracts.

Letki, L., Tang, J., Inyang, C., Du X. and Fletcher, R.P. 2015a. Depth domain inversion to improve the fidelity of subsalt imaging: a Gulf of Mexico case study, First Break, Vol 33, No 9, 81 – 85.

Letki, L., Darke, K., and Araujo Borges, Y. 2015b. A comparison between time domain and depth domain inversion to acoustic impedance. 85th Annual International Meeting, SEG, Expanded Abstracts, 3376-3380.

Salomons, B., M. Kiehn, J. Sheiman, B. Strawn, and Ten Kroode, F. 2014. High fidelity imaging with least squares migration. 76th EAGE Conference and Exhibition, Extended Abstracts.